Molecular Pharmacology Fast Forward. Published on January 27, 2014 as doi:10.1124/mol.113.091017
This article has not been copyedited and formatted. The final version may differ from this version.

Structure/activity relationships of (M)ANT- and TNP-nucleotides for inhibition of rat soluble guanylyl cyclase $\alpha_1\beta_1$

Stefan Dove, Kerstin Yvonne Danker, Johannes-Peter Stasch,

Volkhard Kaever, Roland Seifert

Department of Medicinal Chemistry II, University of Regensburg, Regensburg, Germany (SD)

Institute of Pharmacology, Hannover Medical School, Hannover, Germany (KYD, VK, RS)

Institute of Cardiovascular Research, Bayer HealthCare, Wuppertal, Germany (JPS)

Research Core Unit Metabolomics, Hannover Medical School, Hannover, Germany (VK)

Primary laboratory of origin: Institute of Pharmacology, Hannover Medical School, Carl-Neuberg-Str. 1, D-30625 Hannover, Germany.

Molecular Pharmacology Fast Forward. Published on January 27, 2014 as DOI: 10.1124/mol.113.091017
This article has not been copyedited and formatted. The final version may differ from this version.

Running title: Inhibitors of soluble guanylyl cyclase

Corresponding author: Dr. Roland Seifert, Institute of Pharmacology, Hannover Medical School, Carl-Neuberg-Str. 1, D-30625 Hannover, Germany. Phone: +49-511-532-2805; Fax: +49-511-532-4081; email: seifert.roland@mh-hannover.de

Number of text pages: 25

Number of tables: 1

Number of Figures: 4

Number of references: 49

Number of words in the Abstract: 250

Number of words in the Introduction: 609

Number of words in the Discussion: 1325

Abbreviations: pGC, particulate guanylyl cyclase; sGC, soluble guanylyl cyclase; TNP-NTP, 2',3'-O-(2,4,6-trinitrophenyl)-nucleoside 5'-triphosphate; mAC, membranous adenylyl cyclase; (M)ANT-NTP; 2',3'-O-(N-(methyl)anthraniloyl) nucleoside 5'-triphosphate

Molecular Pharmacology Fast Forward. Published on January 27, 2014 as DOI: 10.1124/mol.113.091017
This article has not been copyedited and formatted. The final version may differ from this version.

Abstract

Soluble guanylyl cyclase (sGC) plays an important role in cardiovascular function and catalyzes formation of cGMP. sGC is activated by nitric oxide and allosteric stimulators and activators. However, despite its therapeutic relevance, the regulatory mechanisms of sGC are still incompletely understood. A major reason for this situation is that no crystal structures of active sGC have been resolved so far. An important step towards this goal is the identification of high-affinity ligands that stabilize a sGC conformation resembling the active, "fully closed" state. Therefore, we examined inhibition of rat sGC $\alpha_1\beta_1$ by 38 purine and pyrimidine nucleotides with 2,4,6,-trinitrophenyl- and (N-methyl)anthraniloyl substitutions at the ribosyl moiety and compared the data with those for the structurally related membranous ACs (mACs) 1, 2 and 5 and the purified mAC catalytic subunits VC1:IIC2. 2',3'-O-(2,4,6-Trinitrophenyl)-guanosine 5'-triphosphate (TNP-GTP) was the most potent sGC $\alpha_1\beta_1$ inhibitor (K_i, 10.7 nM), followed by 2'-O-(N-methylanthraniloyl)-3'-deoxy-adenosine 5'-triphosphate (2'-MANT-3'-dATP) (K_i, 16.7 nM). Docking studies on a sGCαcat/sGCβcat model derived from the inactive heterodimeric crystal structure of the catalytic domains point to similar interactions of MANT- and TNP-nucleotides with sGC $\alpha_1\beta_1$ and mAC VC1:IIC2. Reasonable binding modes of 2'-MANT-3'-dATP and bis-(M)ANT-nucleotides at sGC $\alpha_1\beta_1$ require a 3'-endo ribosyl conformation (vs. 3'-exo in 3'-MANT-2'-dATP). Overall, inhibitory potencies of nucleotides at sGC $\alpha_1\beta_1$ vs. mACs 1, 2 and 5 correlated poorly. Collectively, we identified highly potent sGC $\alpha_1\beta_1$ inhibitors that may be useful for future crystallographic and fluorescence spectroscopy studies. Moreover, it may become possible to develop mAC inhibitors with selectivity relative to sGC.

Molecular Pharmacology Fast Forward. Published on January 27, 2014 as DOI: 10.1124/mol.113.091017
This article has not been copyedited and formatted. The final version may differ from this version.

Introduction

Soluble guanylyl cyclase (sGC) is activated by nitric oxide (NO) and plays an important role in the regulation of cardiovascular and neuronal functions (Friebe et al., 2009; Kots et al., 2011; Derbyshire and Marletta, 2012). Binding of NO to the heme moiety of the enzyme induces a conformational change so that sGC then effectively catalyzes the conversion of GTP into the second messenger cGMP (Friebe et al., 2009; Kots et al., 2011; Derbyshire and Marletta, 2012). NO-containing drugs are used clinically to improve symptoms in coronary heart disease (Daiber et al., 2010). However, a major problem in the clinical use of NO-containing drugs is desensitization, rendering long-term therapy difficult (Daiber et al., 2010). The more recently developed allosteric sGC activators and sGC stimulators are devoid of this serious problem and have substantial potential for the treatment of various cardiovascular diseases including pulmonary hypertension and heart failure (Gheorghiade et al., 2013; Stasch et al., 2013; Follmann et al., 2013). Despite its profound therapeutic relevance, the molecular regulatory mechanisms of sGC function are still incompletely understood (Baskaran et al., 2011; Kumar et al., 2013; Underbakke et al., 2013).

The active sGC holoenzyme is a heterodimer formed by the two subunits sGCα and sGCβ. The catalytic sGC domains, sGCαcat and sGCβcat, are closely related to the catalytic domains of membranous ACs (mACs), C1 and C2, respectively (Sunahara et al., 1998; Seifert et al., 2012). Recently, crystal structures of a sGCβcat homodimer and a sGCαcat/sGCβcat heterodimer have been resolved (Allerston et al., 2013) which, however, represent catalytically inactive, "open" conformations. In contrast, the "fully closed" active state of mACs is well known from several structures of the heterodimeric hybrid VC1:IIC2 (Tesmer et al., 1997, 2000). A major technical advance in the resolution of crystal structures of VC1:IIC2 was achieved by the use of high-affinity competitive mAC inhibitors, i.e. 2',3'-O-(2,4,6-trinitrophenyl) (TNP)- and 2',3'-O-(N-methylanthraniloyl) (MANT)-substituted nucleoside 5'-triphosphates as stabilizing ligands (Mou et al., 2005, 2006; Hübner et al., 2011). These nucleotides bind to the catalytic site of VC1:IIC2, and the TNP- or MANT group projects into a pocket adjacent to the catalytic site, conferring high affinity of the ligands for mACs and stabilizing inactive mAC conformations between the open and closed states (Mou et al., 2005, 2006; Hübner et al., 2011; Seifert et al., 2012). Hydrophobic interactions of the TNP- or MANT-nucleotides were also explored to monitor conformational changes in mACs by fluorescence spectroscopy, providing major new insights into the dynamics of enzyme

Molecular Pharmacology Fast Forward. Published on January 27, 2014 as DOI: 10.1124/mol.113.091017
This article has not been copyedited and formatted. The final version may differ from this version.

regulation (Mou et al., 2005, 2006; Hübner et al., 2011; Pinto et al., 2009, 2011; Suryanarayana et al., 2009).

In previous studies we showed that several TNP- and (M)ANT-nucleotides are potent inhibitors of sGC conventionally purified from bovine lung (Gille et al., 2004; Suryanarayana et al., 2009). The most potent inhibitor of bovine sGC is TNP-ATP (K_i, 7.3 nM) (Suryanarayana et al., 2009). However, for mechanistic and biophysical studies, the recombinant enzyme rat sGC $\alpha_1\beta_1$ is much better suited (Hoenicka et al., 1999, Stasch et al., 2001; Beste et al., 2012). In addition, since we completed our previous inhibitor studies on bovine sGC (Gille et al., 2004; Suryanarayana et al., 2009), various new (M)ANT-nucleotides were developed and characterized at ACs 1, 2 and 5 (Geduhn et al., 2011). All these data prompted us to systematically characterize the interaction of recombinant rat sGC $\alpha_1\beta_1$ with a series of 38 TNP- and (M)ANT-nucleotides with the goal to identify high-affinity inhibitors. Figure 1 shows the structures of the compounds studied. Moreover, based on the availability of crystal structures of sGCαcat/sGCβcat and mAC VC1:IIC2 (Allerston et al., 2013; Tesmer et al., 1997; Mou et al., 2005), we performed docking studies on a rat sGC $\alpha_1\beta_1$ model.

Materials and Methods

Materials. Guanosine 5'-triphosphate (GTP, ≥ 95%), triethylamine (TEA), phosphocreatine, creatine kinase, dithiothreitol (DTT), ethylene glycol bis(2-aminoethyl ether)-N,N,N',N'-tetraacetic acid (EGTA), sodium nitroprusside (SNP), sodium acetate, and bovine serum albumin (BSA) purchased from Sigma-Aldrich (Seelze, Germany). 3'-(N-Methyl-anthraniloyl)-2'-deoxy-adenosine-5'-triphosphate (3'-MANT-2'-dATP), 2'-O-(N-methyl-anthraniloyl)-3'-deoxy-adenosine-5'-triphosphate (2'-MANT-3'-dATP), 2',3'-O-trinitrophenyl-adenosine-5'-triphosphate (TNP-ATP), 2',3'-O-trinitrophenyl-guanosine-5'-triphosphate (TNP-GTP), 2',3'-O-trinitrophenyl-cytosine-5'-triphosphate (TNP-CTP), 2',3'-O-trinitrophenyl-uridine-5'-triphosphate (TNP-UTP), 2',3'-O-(N-methyl-anthraniloyl)-adenosine-5'-[(α,β)-imido]triphosphate (MANT-AppNHp), 2',3'-O-(N-methyl-anthraniloyl)-guanosine-5'-[(α,β)-imido]triphosphate (MANT-GppNHp), 2',3'-O-(N-methyl-anthraniloyl)-adenosine-5'-(thio)-triphosphate (MANT-ATPγS), 2',3'-O-(N-methyl-anthraniloyl)-guanosine-5'-(thio)-triphosphate (MANT-GTPγS), and 2',3'-O-(N-methyl-anthraniloyl)-inosine-5'-(thio)-triphosphate (MANT-ITPγS) were obtained from Jena Bioscience (Jena, Germany). 2',3'-(N-Methyl-anthraniloyl)-inosine-5'-triphosphate (MANT-ITP), 2',3'-(N-methyl-anthraniloyl)-

Molecular Pharmacology Fast Forward. Published on January 27, 2014 as DOI: 10.1124/mol.113.091017
This article has not been copyedited and formatted. The final version may differ from this version.

cytosine-5'-triphosphate (MANT-CTP), 2',3'-(N-methyl-anthraniloyl)-uridine-5'-triphosphate (MANT-UTP) and other (M)ANT-nucleotides were synthesized as described (Geduhn et al., 2011). cGMP (cGMP·Na) was supplied by Biolog (Bremen, Germany). Manganese chloride tetrahydrate, hydrochloric acid, and ammonium acetate were purchased from Fluka (Buchs, Germany). Acetonitrile, methanol and water were supplied by Baker (Deventer, The Netherlands) and acetic acid was purchased from Riedel-de Haën (Seelze, Germany). Tenofovir was obtained through the National Institute of Health AIDS Research and Reference Program, Division of AIDS (catalog no. 10199) (Bethesda, MD). Rat sGC $\alpha_1\beta_1$ was purified as described (Beste et al., 2012).

sGC assay. The sGC assay was performed as described recently in detail (Beste et al., 2012). Briefly, assays contained 1 ng of sGC$\alpha_1\beta_1$ per tube, 50 µM GTP, 3 mM $MnCl_2$, 9 mM phosphocreatine, 2 mg/mL creatine kinase, 50 mM TEA pH 7.5, 100 µM EGTA, 1 mM DTT, 1 mg/mL BSA, 100 µM SNP, and 10-30,000 nM of inhibitors **1**-**38** and were incubated at 37°C. After 20 min, assays were stopped with heating at 95 °C for 10 min. After cooling, mixtures were diluted with 97:3 (v/v) water/methanol solution containing 50 mM ammonium acetate, 0.1% (v/v) acetic acid, and 100 ng/mL tenofovir. Denatured protein was precipitated by centrifugation for 10 min at 20,000g. Supernatants were used for quantitation of generated cGMP using HPLC–MS/MS as described (Beste et al., 2012).

Molecular modeling. The recently published (Allerston et al., 2013) crystal structure of a sGCαcat/sGCβcat heterodimer (PDB 3uvj) represents a catalytically inactive, "open" conformation and could therefore not directly be used for docking studies. However, several structures of mAC VC1:IIC2 in complex with MANT- and TNP-nucleotides (PDB 1tl7, 1u0h, 2gvz, 3g82, 2gvd) (Mou et al., 2005, 2006; Hübner et al., 2011) may serve as templates for the generation of a "partially closed" sGC conformation which binds this class of inhibitors. mAC VC1:IIC2 in complex with 3'-MANT-GTP (PDB 1tl7) was selected because of the highest resolution (2.8 Å). The subunits sGCαcat and sGCβcat were provided with missing side chains, with hydrogens and separately fitted to mAC VC1 and IIC2, respectively, by alignment of the backbones of corresponding amino acids being within 3.5 Å around 3'-MANT-GTP in the mAC structure (10 residues in each subunit). This initial sGCαcat/sGCβcat model was still not able to bind MANT- and TNP-nucleotides because of steric hindrance by the sGCαcat β2-

Molecular Pharmacology Fast Forward. Published on January 27, 2014 as DOI: 10.1124/mol.113.091017
This article has not been copyedited and formatted. The final version may differ from this version.

β3 loop. Therefore, the segment 524-KVETIGDAY-532 was individually adapted to the corresponding mAC VC1 segment 434-RIKILGDCY-442. The MANT-nucleotide binding sites of the resulting sGCcat model and the mAC template fit well (root mean square distance, RMSD, of the backbones of the 20 site residues, 0.85 Å). 2'-MANT-3'-dATP, TNP-GTP and bis-MANT-ITP were manually docked into the sGCcat model based on the binding modes of 3'-MANT-GTP and TNP-GTP in the mAC crystal structures 1tl7 and 2gvd, respectively, and on a previous model of mAC in complex with bis-Br-ANT-ITP (Geduhn et al., 2011). The positions of two Mn^{2+} ions were also adopted from these templates. For 2'-MANT-3'-dATP and bis-Br-ANT-ITP, appropriate docking poses were only obtained with a 3'-endo conformation of the ribosyl moiety. Charges were assigned to the models (proteins and water molecules – AMBER_FF99, ligands – Gasteiger-Hueckel). Mn^{2+} ions received formal charges of 2. Each complex was refined in a stepwise approach. First, 25 minimization cycles with fixed ligand using the AMBER_FF99 force field (Cornell et al., 1995) (steepest descent method); second, 100 minimization cycles of the ligand and the surrounding (distance up to 6 Å) protein residues (Tripos force field) (Clark et al., 1989), third, minimization with fixed ligand (AMBER_FF99 force field, Powell conjugate gradient) and fourth, minimization with fixed protein (Tripos force field) until a root-mean-square force of 0.01 kcal/mol × $Å^{-1}$ was approached in both latter cases. To avoid overestimation of electrostatic interactions, a distance-dependent dielectric constant of 4 was applied. Modeling, docking and preparation of figures was performed with the molecular modeling package SYBYL 8.0 (Tripos Inc., St. Louis, MO) on an Octane workstation (Silicon Graphics International, Fremont, CA). Molecular surfaces and lipophilic potentials (protein variant with the new Crippen parameter table (Heiden et al., 1993; Ghose et al., 1998)) were calculated and visualized by the program MOLCAD (MOLCAD, Darmstadt, Germany) contained within SYBYL.

Statistics. Data are based on four-nine independent experiments and presented as K_i ± standard error (SE) and pK_i (-log K_i). GraphPad Prism software version 5.01 (San Diego, CA) was applied for nonlinear regression and calculation of K_i, pK_i and SE using the GTP concentration of 50 µM and an K_m value of GTP of 14.2 µM as constants.

Molecular Pharmacology Fast Forward. Published on January 27, 2014 as DOI: 10.1124/mol.113.091017
This article has not been copyedited and formatted. The final version may differ from this version.

Results

Inhibition of sGC by MANT- and TNP nucleotides. As expected from previous studies with bovine sGC (Gille et al., 2004; Suryanarayana et al., 2009), MANT-nucleotides were potent inhibitors of recombinant rat sGC$\alpha_1\beta_1$ (Table 1). Bovine sGC was studied with a much more limited inhibitor set than rat sGC$\alpha_1\beta_1$ (Table 1). However, the pK_i values for this set of inhibitors studied at both sGC isoforms correlated well (Figure 2A). In contrast, despite the structural similarities between sGC$\alpha_1\beta_1$ and mAC VC1:IIC2, inhibitor potencies at the two enzymes were only poorly correlated (Figure 2B). In general, inhibitors were more potent at mAC VC1:IIC2 than at sGC$\alpha_1\beta_1$, MANT-XTP (**4**), 2'-MANT-3'-dATP (**7**), TNP-ATP (**22**) and TNP-GTP (**23**) being notable exceptions. The correlations of pK_i values for sGC$\alpha_1\beta_1$ versus mAC2 (Figure 2C), mAC5 (Figure 2D) and mAC1 inhibition, respectively, were not strong. Moderate sGC$\alpha_1\beta_1$ selectivity was observed in the case of MANT-XTP (**4**), 2'-MANT-3'-dATP (**7**), Cl-ANT-ATP (**13**, only mAC2), AcNH-ANT-ATP (**18**), TNP-GTP (**23**) and bis-Pr-ANT-ATP (**35**). By contrast, all ITP derivatives showed high mAC selectivity due to low inhibitory activity in the sGC$\alpha_1\beta_1$ assay.

At sGC$\alpha_1\beta_1$, adenine and xanthine were the preferred bases when MANT-nucleotides were considered (**1**, **5** → **2**-**4**, **6**; **9** → **10**, **11**; **13** → **14**). However, among bis-(M)ANT-nucleotides (**26**-**38**) this preference for adenine was not evident anymore. The triphosphate chain was important for high inhibitor potency (**27** → **29** → **30**). sGC$\alpha_1\beta_1$ did not show striking preference for purines relative to pyrimidines (**1**-**6**; **22**-**25**; **26**-**28**). Removal of the 3'-OH group from the ribosyl moiety, fixing the MANT group in the 2'-position, increased the potency of MANT-ATP about 10-fold (**1** → **7**), whereas removal of the 2'-OH group, fixing the MANT-group in the 3'-position, decreased the potency more than 4-fold. Presumably, both effects are not simply due to the isomerization of the MANT substituent in MANT-ATP (eutomer-distomer ratio ≤ 2 in this case), but should be based on a direct unfavorable or favorable influence of the 2'- and the 3'-OH group, respectively. Substitution of the triphosphate chain by a bulkier γ-thiophosphate chain (**1** → **9**, **2** → **10**, **3** → **11**) had no major impact on inhibitor potency. Exchange of triphosphate against β,γ-imidiodiphosphate did moderately decrease potency in case of guanine (**3** → **21**) but not in case of adenine (**1** → **20**). Substitution of MANT by the smaller ANT group (**1** → **12**) had little effect. Introduction of 5-Cl into ANT increased the affinity in case of adenine about 4-fold (**1** → **13**), whereas larger substitutions in 5-position (propyl, **16**) had no effect or even decreased potency

Molecular Pharmacology Fast Forward. Published on January 27, 2014 as DOI: 10.1124/mol.113.091017
This article has not been copyedited and formatted. The final version may differ from this version.

($AcNH_2$, **18**). In case of hypoxanthine, 5-substituted ANT groups (Cl, **14**, Br, **15**, Pr, **17** or $AcNH_2$, **19**) did not yield inhibitors with higher affinity. Compared to the corresponding MANT-nucleotides, TNP-nucleotides were considerably more potent inhibitors of sGC$\alpha_1\beta_1$ (**1** → **22**; **3** → **23**; **5** → **24**; **6** → **25**). In case of MANT-nucleotides, guanine was preferred relative to adenine (**1** → **3**), whereas the opposite was true for TNP-nucleotides (**22** → **23**). Introduction of a second (substituted) (M)ANT group had no major impact on inhibitor affinity or slightly decreased inhibitor affinity in several cases (**1** → **26**; **2** → **27**; **5** → **28**; **14** → **32**; **15** → **34**; **17** → **36**; **19** → **38**). In some cases with adenine (**16** → **35**; **18** →**37**), the second substituted (M)ANT group led to a more pronounced decrease of inhibitor affinity.

Docking studies of nucleotide inhibitors to an sGCα1β1 model. Based on the recently published (Allerston et al., 2013) crystal structure of an sGCαcat/sGCβcat heterodimer in a catalytically inactive, "open" conformation (PDB 3uvj), a model of a MANT-nucleotide binding state was generated using the complex of mAC VC1:IIC5 with 3'-MANT-GTP (PDB 1tl7) as template (Mou et al., 2005). When bound to mAC VC1:IIC5, the MANT group acts as a wedge between β1-α1-α2 of VC1 and β7'-β8' of IIC2, preventing the formation of the "fully closed", catalytically active conformation (Mou et al., 2005). It is very reasonable to suggest similar binding modes of (M)ANT nucleotides to mAC and sGC by the following reasons: (i) Without the hypoxanthine derivatives with explicit causes of mAC selectivity (hydrogen bonds of the base with Lys938 and Asp1018 (Hübner et al., 2011), replaced by Glu473 and Cys541, respectively, in sGCβ), the correlations of sGC and mAC pK_i-values (Figure 2) substantially increase (sGC vs. mAC1: r, 0.62, vs. mAC2: r, 0.68, mAC5: r, 0.67). (ii) The pK_i scales of the mAC and sGC assays are similar even in the case of more bulky bis-(M)ANT derivatives, there is no "selectively inactive" compound. (iii) Among the 20 amino acids being within 3.5 Å around 3'-MANT-GTP in the mAC VC1:IIC5 structure, only eight are different in sGC (mostly conservative substitutions, VC1 Ala404 vs. sGCα Cys494, Ala409 vs. Pro499, Val413 vs. Ile503, Leu438 vs. Ile528, IIC2 Lys938 vs. sGCβ Glu473, Asp1018 vs. Ser541, Ile1019 vs. Leu542, Trp1020 vs. Phe543).

Based on the fit of these 20 amino acids, a sGCαcat/sGCβcat model resulted that differs from the crystal structure of the inactive state mainly by a 27° rigid body rotation and a translocation of the α subunit (Figure 3A). The close analogy with mAC VC1:IIC5 and in particular of the corresponding MANT-nucleotide binding sites become obvious (Figure 3B).

Molecular Pharmacology Fast Forward. Published on January 27, 2014 as DOI: 10.1124/mol.113.091017
This article has not been copyedited and formatted. The final version may differ from this version.

A model of the fully closed sGC state generated by Allerston et al. (2013) using mAC VC1:IIC5 in complex with ddATP as template (Tesmer et al., 1997) is similar to our model. In this case, the best fit with catalytically active mAC was obtained by a translocation and 26° rotation of sGCα.

Figure 3 shows the pseudosymmetric quaternary structure of MANT-nucleotide bound sGCαcat/sGCβcat. The active site is occupied by 2'-MANT-3'-dATP. A mirror-image site, binding forskolin in various mAC crystal structures (Figure 3B), is potentially suited to interact with allosteric modulators which may be nucleotide derivatives, too (Beste et al., 2012). Both sites together form a deep and spacious cavity between the α- and the β-subunit. The MANT-nucleotide binding site consists of amino acids of the β1-α1-α2 motif and the β2-β3 loop of sGCα as well as of the β1 strand, the β2-β3 loop, the β5 strand, the α4 helix and the β6-β7 loop of sGCβ. In detail, the MANT substituent interacts with sGCα α1-α2 and sGCβ α4, the ribosyltriphosphate moiety with sGCα β1-α1, sGCα β2-β3, sGCβ α4 and sGCβ β6-β7, and the nucleotide base with sGCα β2-β3, sGCβ β1, sGCβ β2-β3, sGCβ β5 and sGCβ α4. Two Mn^{2+} ions were transferred from the mAC template. They coordinate the triphosphate chain and two aspartates in sGCα β1 and β2-β3, respectively.

Figure 4 represents the putative binding modes of three potent sGC inhibitors of different types from Table 1, 2'-MANT-3'-dATP (**7**, Figure 4A), TNP-GTP (**23**, Figure 4B) and bis-MANT-ITP (**27**, Fig. 4C). Since the docking poses of the triphosphate groups were derived from the mAC templates (Mou et al., 2005, 2006; Hübner et al., 2011), the given conformations are only exemplary. The great flexibility of the triphosphate chain, of the surrounding residues and of the Mn^{2+} positions enable different fits with, however, conserved interactions. Each Mn^{2+} ion coordinates sGCα Asp486 and Asp530 as well as two of the phosphate groups (α- plus β- and β- plus γ-phosphate, respectively). One Mn^{2+} is additionally coordinated with the backbone oxygen of sGCα Ile487 (not shown). The phosphate groups form salt bridges with sGCβ Arg552 and Lys593. Apart from putative hydrogen bonds of the ring oxygen with the backbone-NH of Asp530 (not shown), the ribosyl moieties of the three ligands are not involved in specific interactions with sGC, but in hydrophobic contacts with sGCα Phe490.

The low base selectivity of sGC (see Table 1, **2**-**6** and **22**-**25**) may be explained by the spacious, rather unspecific binding pocket between sGCα and sGCβ which is mainly hydrophobic (Fig. 4D) due to residues sGCβ Phe424, Leu542, Val547 and Phe543. Singular

Molecular Pharmacology Fast Forward. Published on January 27, 2014 as DOI: 10.1124/mol.113.091017
This article has not been copyedited and formatted. The final version may differ from this version.

Value Decomposition (SVD) analysis of K_i values of MANT- and TNP-nucleotides indicated that the base contributed less to mAC binding compared to the triphosphate and the MANT or TNP groups (Mou et al., 2006). ATP selectivity of mAC VC1:IIC2 obviously results from hydrogen bonds of the adenine base with Lys938 and Asp1018 (Tesmer et al., 1999). The same residues account for the hypoxanthine selectivity in the case of MANT nucleotides (Hübner et al., 2011). Replacement by sGCβ Glu473 and Cys541 is suggested to determine the GTP selectivity of sGC by hydrogen bonds with two nitrogens (N1, N6) and the oxygen, respectively, of guanine (Sunahara et al., 1998; Allerston et al., 2013). However, both residues do not form specific interactions with the bases in our models, indicating that the binding modes of nucleotides are more or less different from those of their MANT and TNP derivatives. Such differences were also observed for mAC binding of ATP and 3'-MANT-ATP which does not interact with Lys938 and Asp1018 and holds the adenine ring in a *syn* orientation with respect to the ribosyl moiety (Mou et al., 2005). In our models, only the adenine base of 2'-MANT-3'-dATP may form a specific interaction, namely a hydrogen bond of the 6-NH_2 group with the side chain oxygen of sGCβ Thr474. All other interactions of the bases with sGC are hydrophobic and/or of the van der Waals type.

Derived from the binding modes of 3'-MANT-ATP and 3'-MANT-GTP to mAC VC1:IIC2 (Mou et al., 2005, 2006), the 2'-MANT groups of 2'-MANT-3'-dATP and bis-MANT-ITP as well as the TNP group of TNP-GTP are suggested to act as wedges between α1-α2 of sGCα on one and α4 as well as β6-β7 of sGCβ on the other side (Fig. 3). With a 3'-MANT substituent, the ribosyl moiety exists in a 2'-endo envelope conformation (Mou et al., 2005), leading to an equatorial orientation of the 2'-hydroxyl incompatible with binding of a 2'-MANT substituent (strong sterical clashes with mAC VC1). However, like in the case of mAC, docking of 2'-(M)ANT-NTPs to sGC is possible if the ribosyl moiety adopts a 3'-endo envelope conformation enabling an axial 2'- and an equatorial 3'-substituent. Thereby the 2'-MANT groups of 2'-MANT-3'-dATP and bis-MANT-ITP are aligned with the 3'-MANT moiety of mAC-bound 3'-MANT-ATP and -GTP. Moreover, equatorial orientation of the 3'-MANT group in bis-MANT-ITP facilitates interaction with an additional binding pocket between α1 of sGCα and α4 as well as β6-β7 of sGCβ (Figure 4C).

The 2'-MANT substituents and the corresponding TNP group interact with sGCα Phe490, Thr491, Cys494, Pro499, Val502 and Ile503 as well as with sGCβ Phe543, Asn545 and Asn548. Both asparagine side chains are potential donors in hydrogen bonds either with

Molecular Pharmacology Fast Forward. Published on January 27, 2014 as DOI: 10.1124/mol.113.091017
This article has not been copyedited and formatted. The final version may differ from this version.

the 2'-MANT nitrogen (Figure 4A) or with one of the *ortho* nitro substituents in TNP derivatives (Figure 4B). These interactions may be a reason for the substantially higher potency of 2'-MANT-3'-dATP compared to its positional isomer 3'-MANT-2'-dATP (Table 1) because corresponding hydrogen bonds with Asn1025 and Asn1028 are not possible in the structure of mAC VC1:IIC2 complexed with 3'-MANT-ATP (Mou et al., 2005). The docking mode of 2'-MANT-3'-dATP requires a 3'-desoxy position since a 3'-hydroxyl would clash with the side chain of Asn548. I.e., 2'-MANT-ATP, one of the isomers of **1**, is less potent than 2'-MANT-3'-dATP. By contrast, the effect of a 2'-hydroxyl seems to be favorable in both sGC and mACs (compare **1** and **8**) although the structure of mAC VC1:IIC2 does not show direct 2'-OH protein interactions. Definite reasons for the common sGC vs. mAC VC1:IIC2 selectivity of TNP derivatives cannot be derived from the putative docking mode of TNP-GTP (Figure 4B) since the suggested NO_2-Asn hydrogen bonds are generally possible in the case of mAC, too, but not present in the corresponding crystal structure (Mou et al., 2005). In all of the mAC VC1:IIC2 structures in complex with MANT- and TNP-nucleotides, internal water molecules apparently do not contribute to binding of the substituents.

Phe490 of sGCα, corresponding to Phe400 of mAC VC1, seems to play a key role in the binding modes of the three ligands in Figure 4. Its phenyl ring may interact face-to-edge with the 2'-MANT group of 2'-MANT-3'-dATP and bis-MANT-ITP and align with the TNP moiety of TNP-GTP. Contacts with the ribosyl functions of all ligands and with the 3'-MANT group of bis-MANT-ITP are present, too. Phe 490 forms something like a hydrophobic edge at the entrance of the 2'-MANT binding pocket (Figure 4D). The 3'-MANT group of bis-MANT-ITP is in additional hydrophobic and/or van der Waals contact with sGCα Thr 491 and Cys 494 as well as with sGCβ Asn548 and Lys 593. The side chain of Arg 552 (sGCβ) may form a hydrogen bond with the aminomethyl substituent.

Discussion

In this study, we have identified a number of potent inhibitors of sGC$\alpha_1\beta_1$, 2'-MANT-3'-dATP (**7**) and TNP-GTP (**23**) being the most notable compounds (Table 1). These compounds may be useful for future crystallographic and fluorescence spectroscopy studies with sGC$\alpha_1\beta_1$. By analogy to previous studies with mAC VC1:IIC2 (Mou et al., 2006, 2006; Pinto et al., 2009, 2011; Suryanarayana et al., 2009), such biophysical studies with sGC$\alpha_1\beta_1$ are expected to provide major insights into the molecular mechanisms underlying sGC

Molecular Pharmacology Fast Forward. Published on January 27, 2014 as DOI: 10.1124/mol.113.091017
This article has not been copyedited and formatted. The final version may differ from this version.

regulation by NO, sGC activators and sGC stimulators (Stasch et al., 2013; Follmann et al., 2013; Daiber et al., 2010; Derbyshire et al., 2012). In fact, Busker et al. has recently reported on the application of MANT-nucleotides for monitoring conformational changes in sGC upon activation (Busker et al., 2014). While most compounds examined here exhibited lower potency at sGC$\alpha_1\beta_1$ than at mAC VC1:IIC2 and mACs 1, 2 and 5 (Table 1), the striking preference of sGC$\alpha_1\beta_1$ for 2'-MANT-3'-dATP points to some unique structural features in the latter enzyme, indicating that development of potent and selective sGC inhibitors is feasible. In case of *Bacillus anthracis* edema factor AC toxin, defined 2'- and 3'-isomers of MANT-nucleotides turned out to be exceptionally valuable tools for probing conformational states (Seifert and Dove, 2013). Due to the base preference of sGC$\alpha_1\beta_1$ among MANT-nucleotides (Table 1), 2'-MANT-3'-dXTP is predicted to constitute a particularly potent sGC$\alpha_1\beta_1$ inhibitor.

Our present sGC$\alpha_1\beta_1$ inhibitor data should also be viewed from the perspective of mAC inhibitors. Specifically, it has been suggested that selective AC5 inhibitors may be valuable drugs for the treatment of heart failure (Vatner et al., 2013). However, it is difficult to develop highly selective AC5 inhibitors (Bräunig et al., 2013; Brand et al., 2013; Seifert, 2014), and in context with heart failure, additional inhibition of sGC would be detrimental for cardiovascular function (Schemuly et al., 2011; Gheorghiade et al., 2013). Rather, sGC activation would be desirable (Schemuly et al., 2011; Gheorghiade et al., 2013). In principle, the development of potent AC5 inhibitors with selectivity relative to sGC is feasible, MANT-ITP (**2**, > 400-fold selectivity) and Cl-ANT-ITP (**14**, > 600-fold selectivity) providing good starting points (Table 1). This is a very promising result for future research in this field since in the present study, we investigated only a small set of compounds (< 40), and nonetheless, achieved selectivity for AC5 relative to sGC$\alpha_1\beta_1$. Smilarly, selectivity for ACs 1 and 2 relative to sGC$\alpha_1\beta_1$ is possible (Table 1 and Figure 2). Selectivity of inhibitors among various mAC isoforms is probably more difficult to achieve (Seifert et al., 2012; Bräunig et al., 2013; Brand et al., 2013; Seifert, 2014).

The fact that not only purine- but also pyrimidine nucleotides inhibited sGC$\alpha_1\beta_1$ was not surprising in view of the finding that UTP and CTP are also substrates for this enzyme both at the level of the purified enzyme and at the intact cell level (Beste et al., 2012; Bähre et al., 2014). Purine- and pyrmidine nucleotides are also quite potent mAC inhibitors (Gille et al., 2004; Mou et al., 2005, 2006; Hübner et al., 2011; Pinto et al., 2011; Suryanarayana et al., 2009), but currently, it is not known whether mACs also accept UTP and CTP as

Molecular Pharmacology Fast Forward. Published on January 27, 2014 as DOI: 10.1124/mol.113.091017
This article has not been copyedited and formatted. The final version may differ from this version.

substrates. This will be an important research topic for future studies considering the fact that mammalian cells endogenously contain substantial concentrations of 3',5'-cCMP and 3',5'-cUMP and that sGC produces these cyclic pyrimidine nucleotides in intact cells (Beste et al., 2013; Bähre et al., 2014).

In a recent study, we have identified bis-Cl-ANT-ATP as a highly potent inhibitor of *Bordetella pertussis* CyaA AC toxin with > 100-fold selectivity relative to mACs 1, 2 and 5 (Geduhn et al., 2011). Bis-Cl-ANT-ATP is a valuable starting point for the development of CyaA inhibitors that are of potential value in the treatment of whooping cough (Seifert and Dove, 2012). Selectivity of bis-Cl-ANT-ATP for CyaA relative for sGC$\alpha_1\beta_1$ is also quite good (> 30-fold), and it is possible that introduction of other bases than adenine or hypoxanthine further improves CyaA-selectivity. In contrast to the situation with CyaA, we have not observed a situation for sGC$\alpha_1\beta_1$ where introduction of a second (M)ANT substitutent into the inhibitor increased affinity, indicating a more constrained catalytic site in sGC$\alpha_1\beta_1$ than in CyaA.

TNP-nucleotides are similarly potent sGC- and mAC inhibitors (Table 1). Thus, in terms of nucleotidyl cyclase isoform-selectivity, the TNP group is not favorable. However, TNP-nucleotides monitor different conformational changes in mACs than MANT-nucleotides (Suryanarayana et al., 2009). Considering the high affinity of sGC$\alpha_1\beta_1$ for TNP-CTP and TNP-UTP, these nucleotides may become particularly valuable tools for answering the question why UTP and CTP are good sGC substrates in the presence of Mn^{2+} but not in the presence of Mg^{2+} (Beste et al., 2012).

Although, in general, both sGC and mACs exhibit broad base-promiscuity (Table 1) (Gille et al., 2004; Mou et al., 2005, 2006; Hübner et al., 2011; Pinto et al., 2011; Suryanarayana et al., 2009), there are some striking differences, specifically with respect to purine bases. In case of mACs, hypoxanthine is the preferred base, and accordingly, MANT-ITP is the most potent mAC inhibitor known so far (Hübner et al., 2011). In contrast, MANT-XTP exhibits only low affinity for mAC (Mou et al., 2005; Hübner et al., 2011), whereas in case of sGC, xanthine is preferred relative to hypoxanthine. This differential inhibition of nucleotidyl cyclases by nucleotides possessing different purine bases will be important for future studies on isoform-selectivity of inhibitors.

The major sGC isoform in lung is sGC$\alpha_1\beta_1$ (Koesling et al., 1990; Harteneck et al., 1991). Conventionally purified bovine lung sGC$\alpha_1\beta_1$ (Humbert et al., 1990) and recombinant

Molecular Pharmacology Fast Forward. Published on January 27, 2014 as DOI: 10.1124/mol.113.091017
This article has not been copyedited and formatted. The final version may differ from this version.

rat cGC$\alpha_1\beta_1$ (Hoenicka et al., 1999) exhibit a similar pharmacological inhibition profile (Table 1). Therefore, it appears that in case of sGC, species-selectivity of inhibitors is not a major issue. In contrast, other signal transduction proteins from bovine and rat, specifically histamine receptors, show striking species-selectivity (Strasser et al., 2013). To this end, species-specificity of mAC inhibitors has not yet been studied, but it should be noted that the most commonly studied mACs, i.e. mACs 1, 2 and 5, were cloned from different species (Gille et al., 2004).

In contrast to sGC, the atrial natriuretic peptide-stimulated pGC-A does not accept UTP or CTP as substrates (Beste et al., 2013). Based on this differential substrate-specificity it may also become possible to develop selective pGC inhibitors. To the best of our knowledge MANT-nucleotides have not yet been examined at pGC. However, such studies are worthwhile, and we expect a different inhibitor profile for pGC compared to sGC and mACs. First steps towards the development of selective allosteric pGC modulators have already been taken (Robinson and Potter, 2012; Seifert and Beste, 2012). Identification of high-potency pGC-A inhibitors may support biophysical studies with this enzyme.

In conclusion, here, we have presented a comprehensive structure/activity relationship study for sGC inhibitors. We have obtained several potent sGC inhibitors that could be used as experimental tools for fluorescence spectroscopy and crystallographic studies. Docking of representative inhibitors into a sGCαcat/sGCβcat model has provided binding modes accounting for the high affinity of derivatives from different structural classes and suggesting some possible reasons for their sGC vs. mAC selectivity. Based on our data, the rational development of even more potent sGC inhibitors is possible. With respect to treatment of cardiovascular diseases, inhibition of mAC5 may be desirable, whereas sGC inhibition is not. Our present study also provides guidelines for the development of potent mAC5 inhibitors with low affinity for sGC. Furthermore, CyaA inhibitors may be valuable for the treatment of whooping cough and again, development of CyaA inhibitors with high selectivity relative to sGC is achievable. The crystallization of sGC with one of the inhibitors described in this study will further aid the development of nucleotidyl cyclase inhibitors that do not target sGC because low sGC activity is unfavorable. In other words, the catalytic site of sGC is an antitarget, and the present study characterized this antitarget at the molecular level.

Molecular Pharmacology Fast Forward. Published on January 27, 2014 as DOI: 10.1124/mol.113.091017
This article has not been copyedited and formatted. The final version may differ from this version.

Acknowledgements

The authors would like to thank Prof. Dr. Burkhard König and Dr. Jens Geduhn for providing several (M)ANT-nucleotides and Mrs. Annette Garbe for expert technical assistance.

Author contributions

Participated in research design: Dove, Danker, Seifert

Contributed to new reagents and analytical tools: Stasch, Kaever

Performed data analysis: Dove, Danker, Seifert

Wrote or contributed to writing of the manuscript: Dove, Danker, Stasch, Kaever, Seifert

Molecular Pharmacology Fast Forward. Published on January 27, 2014 as DOI: 10.1124/mol.113.091017
This article has not been copyedited and formatted. The final version may differ from this version.

References

Allerston CK, von Delft F, and Gileadi O (2013) Crystal structures of the catalytic domain of human soluble guanylate cyclase. *Plos One* **8:** e57644.

Bähre H, Danker KY, Stasch JP, Kaever V, and Seifert R (2014) Nucleotidyl cyclase activity of soluble guanylyl cyclase in intact cells. *Biochem Biophys Res Commun* PMID24380860.

Baskaran P, Heckler EJ, van den Akker F, and Beuve A (2011) Identification of residues in the heme domain of soluble guanylyl cyclase that are important for basal and stimulated catalytic activity. *PLoS One* **6:** e26976.

Beste KY, Burhenne H, Kaever V, Stasch JP, and Seifert R (2012) Nucleotidyl cyclase activity of soluble guanylyl cyclase $\alpha_1\beta_1$. *Biochemistry* **51:** 194-204.

Beste KY, Spangler CM, Burhenne H, Koch KW, Shen Y, Tang WJ, Kaever V, and Seifert R (2013) Nucleotidyl cyclase activity of particulate guanylyl cyclase A: comparison with particulate guanylyl cyclases E and F, soluble guanylyl cyclase and bacterial adenylyl cyclases CyaA and edema factor. *PLoS One* **8:** e70223.

Brand CS, Hocker HJ, Gorfe AA, Cavasotto CN, and Dessauer CW (2013) Isoform selectivity of adenylyl cyclase inhibitors: characterization of known and novel compounds. *J Pharmacol Exp Ther* **347:** 265-275.

Bräunig JH, Schweda F, Han PL, and Seifert, R (2013) Similarly potent inhibition of adenylyl cyclase by P-site inhibitors in hearts from wild type and AC5 knockout mice. *PLoS One* **8:** e68009.

Busker M, Neidhardt I, and Behrends S (2014) Nitric oxide activation of guanylate cyclase pushes the α_1 signaling helix and the β_1 heme-binding domain closer to the substrate-binding site. *J Biol Chem* **289:** 476-484.

Clark M, Cramer RDI, and van Opdenbosch N (1989) Validation of the general purpose tripos 5.2 force field. *J Comp Chem* **10:** 982-1012.

Cornell WD, Cieplak P, Bayly CI, Gould IR, Merz KMJ, Ferguson DM, Spellmeyer DC, Fox T, Caldwell JW, and Kollman PA (1995) A second generation force field for the simulation of proteins and nucleic acids. *J Am Chem Soc* **117:** 5179-5197.

Daiber A, Münzel T, and Gori T (2010) Organic nitrates and nitrate tolerance – state of the art and future developments. *Adv Pharmacol* **60:** 177-227.

Derbyshire ER, and Marletta MA (2012) Structure and regulation of soluble guanylyl cyclase. *Annu Rev Biochem* **81:** 533-559.

Follmann M, Griebenow N, Hahn MG, Hartung I, Mais FJ, Mittendorf J, Schäfer M, Schirok H, Stasch JP, Stoll F, Straub A (2013) From explosives to modern medicinal chemistry: The chemistry and pharmacology of soluble guanylate cyclase stimulators and activators. *Angew Chem Int Ed* **52:** 9442-9462.

Friebe A, and Koesling D (2009) The function of NO-sensitive guanylyl cyclase: what we can learn from genetic mouse models. *Nitric Oxide* **21:** 149-156.

Geduhn J, Dove S, Shen Y, Tang WJ, König B, and Seifert R (2011) Bis-halogen-anthraniloyl-substituted nucleoside 5'-triphosphates as potent and selective inhibitors of *Bordetella pertussis* adenylyl cyclase toxin. *J Pharmacol Exp Ther* **336:** 104-115.

Gheorghiade M, Marti CN, Sabbah HN, Roessig L, Greene SJ, Böhm M, Burnett JC, Campia U, Cleland JGF, Collins SP, Fonarow GC, Levy PD, Metra M, Pitt B, Ponikowski P, Sato N, Voors AA, Stasch JP, and Butler J (2013) Soluble guanylate cyclase: a potential therapeutic target for heart failure. *Heart Fail Rev* **18:** 123-134.

Gille A, Lushington GH, Mou TC, Doughty MB, Johnson RA, and Seifert R (2004) Differential inhibition of adenylyl cyclase isoforms and soluble guanylyl cyclase by purine and pyrimidine nucleotides. *J Biol Chem* **279:** 19955-19969.

Ghose AK, Viswanadhan VN, and Wendoloski JJ (1998) Prediction of hydrophobic (lipophilic) properties of small organic molecules using fragmental methods: An analysis of ALOGP and CLOGP methods. *J Phys Chem* **102:** 3762-3772.

Göttle M, Geduhn J, König B, Gille A, Höcherl K, Seifert R, Ko B, and Ho K (2009) Characterization of mouse heart adenylyl cyclase. *J Pharmacol Exp Ther* **329:** 1156-1165.

Harteneck C, Wedel B, Koesling D, Malkewitz J, Böhme E, and Schultz G (1991) Molecular cloning and expression of a new α-subunit of soluble guanylyl cyclase. Interchangeability of the a-subunits of the enzyme. *FEBS Lett* **292:** 217-222.

Heiden W, Moeckel G, and Brickmann J (1993) A new approach to analysis and display of local lipophilicity/hydrophilicity mapped on molecular surfaces. *J Comput Aided Mol Des* **7:** 503-514.

Hoenicka M, Becker EM, Apeler H, Srichoke T, Schröder H, Gerzer R, and Stasch JP (1999) Purified soluble guanylyl cyclase expressed in baculovirus/Sf9 system: stimulation by YC-1, nitric oxide, and carbon monoxide. *J Mol Med* **77:** 14-23.

Hübner M, Dixit A, Mou TC, Lushington GH, Pinto C, Gille A, Geduhn J, König B, Sprang SR, and Seifert R (2011) Structural basis for the high-affinity inhibition of mammalian membranous adenylyl cyclase by 2',3'-O-(N-methylanthraniloyl)-inosine 5'-triphosphate. *Mol Pharmacol* **80:** 87-96.

Humbert P, Niroomand F, Fischer G, Mayer B, Koesling D, Hinsch KD, Gausepohl H, Frank R, Schultz G, Böhme E (1990) Purification of soluble guanylyl cyclase from bovine lung by a new immunoaffinity chromatographic method. *Eur J Biochem* **190:** 273-278.

Koesling D, Harteneck C, Humbert P, Bosserhof A, Frank R, Schultz G, and Böhme E (1990) The primary structure of the larger subunit of soluble guanylyl cyclase from bovine lung. Homology between the two subunits of the enzyme. *FEBS Lett* **266:** 128-132.

Kots AY, Bian K, and Murad F (2011) Nitric oxide and cyclic GMP signalling pathway as a focus for drug development. *Curr Med Chem* **18:** 3299-3305.

Kumar V, Martin F, Hahn MG, Schaefer M, Stamler JS, Stasch JP, and van den Akker F (2013) Insights into BAY 60-2770 activation and S-nitrosylation-dependent desensitization of soluble guanylyl cyclase via crystal structures of homologous Nostoc H-NOX domain complexes. *Biochemistry* **52:** 3601-3608.

Mou TC, Gille A, Fancy DA, Seifert R, and Sprang SR (2005) Structural basis for the inhibition of mammalian membrane adenylyl cyclase by 2'(3')-O-(N-methylanthraniloyl)-guanosine 5'-triphosphate. *J Biol Chem* **280:** 7253-7261.

Mou TC, Gille A, Suryanarayana S, Richter M, Seifert R, and Sprang SR (2006) Broad specificity of mammalian adenylyl cyclase for interaction with 2',3'-substituted purine- and pyrimidine nucleotide inhibitors. *Mol Pharmacol* **70:** 878-886.

Pinto C, Hübner M, Gille A, Richter M, Mou TC, Sprang SR, and Seifert R (2009) Differential interactions of the catalytic subunits of adenylyl cyclase with forskolin analogs. *Biochem Pharmacol* **78:** 62-69.

Pinto C, Lushington GH, Richter M, Gille A, Geduhn J, König B, Sprang SR, and Seifert R (2011) Structure-activity relationships for the interactions of 2'- and 3'-(O)-(N-methyl)anthraniloyl-substituted purine and pyrimidine nucleotides with mammalian adenylyl cyclases. *Biochem Pharmacol* **82:** 358-370.

Robinson JW, and Potter LR (2012) Guanylyl cyclases A and B are asymmetric dimmers that are allosterically activated by ATP binding to the catalytic domain. *Sci Signal* **5:**ra65.

Schemuly RT, Janssen W, Weissmann N, Stasch JP, Grimminger F, and Ghofrani HA (2011) Riociguat for the treatment of pulmonary hypertension. *Expert Opin Invest Drugs* **20:** 567-576.

Schmidt HH, Schmidt PM, and Stasch JP (2009) NO- and haem-independent soluble guanylate cyclase activators. *Handb Exp Pharmacol* **191:** 309-339.

Seifert R (2014) Vidarabine is neither a potent nor a selective AC5 inhibitor. *Biochem Pharmacol* PMID24398424

Seifert R, Lushington GH, Mou TC, Gille A, and Sprang SR (2012) Inhibitors of membranous adenylyl cyclases. *Trends Pharmacol Sci* **33:** 64-78.

Seifert R, and Dove KY (2012) Allosteric regulation nucleotidyl cyclases: an emerging pharmacological target. *Sci Signal* **5:**pe37.

Seifert R, and Dove S (2012) Towards selective inhibitors of adenylyl cyclase toxin from *Bordetella pertussis*. *Trends Microbiol* **20:** 343-351.

Seifert R, and Dove S (2013) Inhibitors of *Bacillus anthracis* edema factor. *Pharmacol Ther* **140:** 200-212.

Stasch JP, Evgenov OV (2013) Soluble guanylate cyclase stimulators in pulmonary hypertension. *Handb Exp Pharmacol* **218:** 279-313.

Stasch JP, Becker EM, Alonso-Alija C, Apeler H, Dembowsky K, Feurer A, Gerzer R, Minuth T, Perzborn E, Pleiss U, Schröder H, Schroeder W, Stahl E, Steinke W, Straub A, and Schramm M (2001) NO-independent regulatory site on soluble guanylyl cyclase. *Nature* **410:** 212-215.

Sunahara RK, Beuve A, Tesmer JJ, Sprang SR, Garbers DL, and Gilman AG (1998) Exchange of substrate and inhibitor specificities between adenylyl and guanylyl cyclases. *J Biol Chem* **273:** 16332-16338.

Suryanarayana S, Göttle M, Hübner M, Gille A, Mou TC, Sprang SR, Richter M, and Seifert R (2009) Differential inhibition of various adenylyl cyclase isoforms and soluble guanylyl cyclase by 2',3'-O-(2,4,6-trinitrophenyl)-substituted nucleoside 5'-triphosphates. *J Pharmacol Exp Ther* **330:** 687-695.

Strasser A, Wittmann HJ, Buschauer A, Schneider EH, Seifert R (2013) Species-dependent activities of G-protein-coupled receptor ligands: lessons from histamine receptor orthologs. *Trends Pharmacol Sci* **34:** 13-32.

Tesmer JJ, Sunahara RK, Gilman AG, and Sprang SR (1997) Crystal structures of the catalytic domains of adenylyl cyclase in a complex with $G_{s\alpha}$.GTPγS. *Science* **278:** 1907-1916.

Tesmer JJ, Sunahara RK, Johnson RA, Gosselin G, Gilman AG, and Sprang SR (1999) Two-metal-ion catalysis in adenylyl cyclase. *Science* **285:** 756-760.

Tesmer JJ, Dessauer CW, Sunahara RK, Murray LD, Johnson RA, Gilman AG, and Sprang SR (2000) Molecular basis for P-site inhibition of adenylyl cyclase. *Biochemistry* **39:** 14464-14471.

Underbakke ES, Iavarone AT, and Marletta MA (2013) Higher-order interactions bridge the nitric oxide receptor and catalytic domains of soluble guanylate cyclase. *Proc Natl Acad Sci USA* **110:** 6777-6782.

Vatner SF, Park M, Yan L, Lee GJ, Lai L, Iwatsubo K, Ishikawa Y, Pessin J, and Vatner DE (2013) Adenylyl cyclase type 5 in cardiac disease, metabolism and aging. *Am J Physiol Heart Circ Physiol* **305:** H1-H8.

Molecular Pharmacology Fast Forward. Published on January 27, 2014 as DOI: 10.1124/mol.113.091017
This article has not been copyedited and formatted. The final version may differ from this version.

Footnotes

Stefan Dove and Kerstin Yvonne Danker contributed equally to this paper.

This work was supported by the Deutsche Forschungsgemeinschaft (Research Training Group 1910; SD and RS).

Reprint requests to: Dr. Roland Seifert, Institute of Pharmacology, Hannover Medical School, Carl-Neuberg-Str. 1, D-30625 Hannover, Germany. Phone: +49-511-532-2805; Fax: +49-511-532-4081; email: seifert.roland@mh-hannover.de

Molecular Pharmacology Fast Forward. Published on January 27, 2014 as DOI: 10.1124/mol.113.091017
This article has not been copyedited and formatted. The final version may differ from this version.

Figure legends

Figure 1. Structures of the 38 nucleotides examined in this study. In this study, (M)ANT-nucleotides (1-21, 26-38) and TNP-nucleotides (22-25) were examined. Nucleotides differed from each other in terms of the base (A, adenine; I, hypoxanthine; G, guanine; X, xanthine; C, cytosine; U, uracil), phosphate chain length (mono-, di- and triphosphate), type of phosphate chain (triphosphate, γ-thiophosphate or β,γ-imidophosphate), 2',3'-O-ribosyl substitution (TNP, MANT, ANT, 5-substituted ANT group, mono- or bis-substitution) and 2'- or 3'-deoxyribosyl group. In nucleotides bearing a 2'-OH- and a 3'-OH group in conjunction with a single (M)ANT group, isomerisation of the substituent between the 2'- and 3'-O-ribosyl position occurs. (M)ANT- and TNP-nucleotides cannot only be used to explore structure/activity relationships of inhibitors at nucleotidyl cyclases, but they can also be applied as fluorescence sensors to monitor conformational changes and as stabilizing ligands for crystallography. For the latter two purposes, the ligands depicted here have not yet been used at sGC$\alpha_1\beta_1$.

Figure 2. Comparison of pK_i values for inhibitors at sGC$\alpha_1\beta_1$ from rat versus sGC from bovine and versus mACs VC1:IIC2, 2 and 5. Dotted lines represent the 99% confidence bands. **A**, Correlation of rat sGC$\alpha_1\beta_1$ with bovine lung sGC (regression through the means); slope, 0.67 ± 0.21; intercept, 2.21 ± 1.42; r, 0.92; $p < 0.0001$. **B-D**, Correlation of rat sGC$\alpha_1\beta_1$ with mACs VC1:IIC2, 2 and 5 (regression through the origin, correlation coefficients r and probabilities of error p from regression through the means). The correlation with mAC1 is not shown because of the high correlation with mAC5 (r, 0.97). Numbered symbols – compounds with striking selectivity for sGC$\alpha_1\beta_1$ (left) and mACs (right), respectively; gray areas – ITP derivatives. **B**, Rat sGC$\alpha_1\beta_1$ vs. mAC VC1:IIC2; slope, 0.89 ± 0.08; r, 0.43; p, 0.087. **C**, Rat sGC$\alpha_1\beta_1$ vs. mAC2; slope, 1.01 ± 0.04; r, 0.33; p, 0.051. **D**, Rat sGC$\alpha_1\beta_1$ vs. mAC5; slope, 0.91 ± 0.04; r, 0.38; p, 0.023. Regression analyses and plots were performed with GraphPad Prism 5.

Figure 3. Schematic overview of the putative (M)ANT- and TNP-nucleotide binding sGCαcat/sGCβcat conformation. α-Helices are drawn as cylinders, β-sheets as arrowed ribbons and loops as tubes. Colors: sGCαcat – cyan, sGCβcat – green. The nucleotide binding site is adopted by 2'-MANT-3'-dATP, represented by a Connolly surface (atom colors: carbon

Molecular Pharmacology Fast Forward. Published on January 27, 2014 as DOI: 10.1124/mol.113.091017
This article has not been copyedited and formatted. The final version may differ from this version.

and hydrogen – yellow, oxygen – red, nitrogen – blue, phosphorus – orange). The magenta-colored balls represent two Mn^{2+} ions. **A**. Comparison of the model with the inactive, "open" conformation of the sGCαcat/sGCβcat crystal structure (PDB 3uvj (Allerston et al., 2013)). The sGCβcat subunits are aligned, whereas the gray subunit displays sGCαcat in the inactive heterodimer. **B**. Alignment of the (M)ANT-nuleotide binding conformations of sGCαcat/sGCβcat and mAC VC1:IIC2 (colors: VC1 – magenta, IIC2 – tan). mAC VC1:IIC2 is represented by the crystal structure PDB 1tl7 (Mou et al., 2005) in complex with 3'-MANT-GTP and forskolin which is additionally shown as transparent space fill model to indicate the position of the second, pseudosymmetric binding site. The fit is based on the 20 mAC VC1:IIC2 amino acids within 3.5 Å around 3'-MANT-GTP.

Figure 4. Models of the interactions of inhibitors with sGC$\alpha_1\beta_1$. Colors of atoms unless otherwise indicated: carbon and hydrogen – gray, oxygen – red, nitrogen – blue, phosphorus – orange, sulfur – yellow, Mn^{2+} – magenta. **A**-**C**: Suggested docking modes of three potent representatives of the structural classes 2'-MANT-, TNP- and bis-MANT-nucleotides. The ligands are drawn as ball and stick, amino acids within 3 Å around as stick models. Carbon, backbone nitrogen and some essential hydrogen atoms as well as schematic backbone tubes are colored by subunit: sGCαcat – cyan, sGCβcat – green. **A**. Docking mode of 2'-MANT-3'-dATP (**7**). **B**. Docking mode of TNP-GTP (**23**). **C**. Docking mode of bis-MANT-ITP (**27**). **D**. Binding site of bis-MANT-ITP, represented by the lipophilic potential mapped onto a MOLCAD Connolly surface (brown, hydrophobic areas, green and blue, polar areas); bis-MANT-ITP is drawn as ball and stick model, bonds and carbon atoms are colored by substructure: triphosphate group – gray, ribosyl moiety – light pink, hypoxanthine – pale blue, 2'-MANT – ochery, 3'-MANT – yellow.

Molecular Pharmacology Fast Forward. Published on January 27, 2014 as DOI: 10.1124/mol.113.091017
This article has not been copyedited and formatted. The final version may differ from this version.

Table 1. Inhibition of rat lung sGC $\alpha_1\beta_1$ by purine and pyrimidine nucleotide analogs: Comparison with bovine sGC, mACs and VC1:IIC2

Cpd.	inhibitor	K_i [nM] sGC $\alpha_1\beta_1$ ± SE	pK_i sGC $\alpha_1\beta_1$	pK_i bovine sGC	pK_i mAC1	pK_i mAC2	pK_i mAC5	pK_i VC1:IIC2
1	MANT-ATP	170 ± 10	6.77	6.37 [a]	6.82 [c]	6.48 [c]	7.00 [c]	7.80 [c]
2	MANT-ITP	500 ± 30	6.31		8.55 [c]	7.85 [c]	8.92 [c]	9.15 [c]
3	MANT-GTP	860 ± 50	6.06	6.15 [b]	7.05 [c]	6.21 [c]	7.28 [c]	7.74 [c]
4	MANT-XTP	110 ± 10	6.95		5.96 [c]	5.52 [c]	5.89 [c]	5.92 [c]
5	MANT-CTP	520 ± 40	6.28		6.82 [c]	6.16 [c]	6.82 [c]	8.04 [c]
6	MANT-UTP	500 ± 50	6.30		7.34 [c]	6.34 [c]	7.49 [c]	8.21 [c]
7	2'-MANT-3'-dATP	17 ± 1	7.78		6.33 [c]	6.27 [c]	7.19 [c]	7.05 [c]
8	3'-MANT-2'-dATP	740 ± 80	6.13	5.44 [a]	6.49 [c]	5.32 [c]	6.44 [c]	6.72 [c]
9	MANT-ATPγS	130 ± 7	6.88		6.80 [d]	6.42 [d]	7.11 [d]	
10	MANT-ITPγS	930 ± 80	6.03	5.31 [b]	7.39 [b]	6.92 [b]	7.51 [b]	7.72 [c]
11	MANT-GTPγS	470 ± 40	6.33	5.96 [b]	7.21 [b]	6.44 [b]	7.46 [b]	7.62 [c]
12	ANT-ATP	240 ± 20	6.63		6.89 [c]	6.19 [c]	6.92 [c]	7.77 [c]
13	Cl-ANT-ATP	47 ± 4	7.33		7.10 [e]	6.31 [e]	7.35 [e]	
14	Cl-ANT-ITP	1,200 ± 100	5.92		8.48 [e]	8.10 [e]	8.70 [e]	
15	Br-ANT-ITP	600 ± 50	6.22		8.15 [e]	7.66 [e]	8.34 [e]	
16	Pr-ANT-ATP	160 ± 10	6.80		6.36 [e]	5.96 [e]	6.44 [e]	
17	Pr-ANT-ITP	390 ± 50	6.41		7.66 [e]	7.17 [e]	8.00 [e]	
18	AcNH-ANT-ATP	780 ± 70	6.11		5.17 [e]	4.96 [e]	5.47 [e]	
19	AcNH-ANT-ITP	600 ± 50	6.22		6.85 [e]	6.41 [e]	7.43 [e]	
20	MANT-AppNHp	170 ± 20	6.77	6.64 [b]	6.80 [b]	6.31 [b]	6.92 [b]	7.70 [b]
21	MANT-GppNHp	2,800 ± 400	5.56	5.82 [b]	6.96 [b]	6.18 [b]	7.01 [b]	7.47 [b]
22	TNP-ATP	21 ± 2	7.67	8.14 [a]	8.05 [a]	7.00 [a]	8.43 [a]	7.09 [f]
23	TNP-GTP	11 ± 1	7.97	8.07 [a]	7.64 [a]	6.66 [a]	7.57 [a]	7.08 [f]
24	TNP-CTP	98 ± 5	7.01	7.57 [a]	7.62 [a]	6.96 [a]	7.51 [a]	6.51 [f]
25	TNP-UTP	51 ± 4	7.29	7.48 [a]	8.15 [a]	7.62 [a]	7.82 [a]	7.04 [f]
26	Bis-MANT-ATP	580 ± 70	6.23		6.15 [e]	5.68 [e]	6.37 [e]	
27	Bis-MANT-ITP	350 ± 20	6.46		6.51 [e]	5.96 [e]	6.85 [e]	
28	Bis-MANT-CTP	790 ± 80	6.10		6.21 [e]	5.11 [e]	6.12 [e]	
29	Bis-MANT-IDP	1,900 ± 100	5.72		6.00 [e]	5.85 [e]	6.15 [e]	
30	Bis-MANT-IMP	>100,000	< 3		< 3 [e]	< 3 [e]	< 3 [e]	
31	Bis-Cl-ANT-ATP	520 ± 50	6.28		5.77 [e]	5.62 [e]	5.80 [e]	
32	Bis-Cl-ANT-ITP	840 ± 60	6.08		7.18 [e]	6.70 [e]	7.19 [e]	
33	Bis-Br-ANT-ATP	430 ± 50	6.37					
34	Bis-Br-ANT-ITP	630 ± 50	6.20		7.68 [e]	7.15 [e]	7.82 [e]	
35	Bis-Pr-ANT-ATP	3,600 ± 300	5.44		4.74 [e]	4.44 [e]	4.74 [e]	
36	Bis-Pr-ANT-ITP	1,200 ± 70	5.91		6.36 [e]	5.85 [e]	6.60 [e]	
37	Bis-AcNH-ANT-ATP	3,900 ± 600	5.41		4.66 [e]	5.15 [e]	5.21 [e]	
38	Bis-AcNH-ANT-ITP	1,100 ± 80	5.97		5.77 [e]	5.25 [e]	6.32 [e]	

sGC activity was determined as described in Materials and Methods and in the presence of Mn^{2+}. Reaction mixtures contained nucleotides analogs at concentrations from 10 nM to 30,000 nM. Inhibition curves were analyzed by nonlinear regression and were best-fitted to monophasic sigmoidal curves. Data for sGC $\alpha_1\beta_1$ were determined in the present study. Data for mACs 1, 2 and 5, VC1:IIC2 and bovine sGC were taken from the literature as follows. [a] Suryanarayana et al., 2009; [b] Gille et al., 2004; [c] Pinto et al., 2011; [d] Göttle et al., 2009; [e] Geduhn et al., 2011; [f] Mou et al., 2006. The structures of the inhibitors examined are shown in Figure 1. The data shown in this Table are the basis for the correlations depicted in Figure 2.

Figure 1

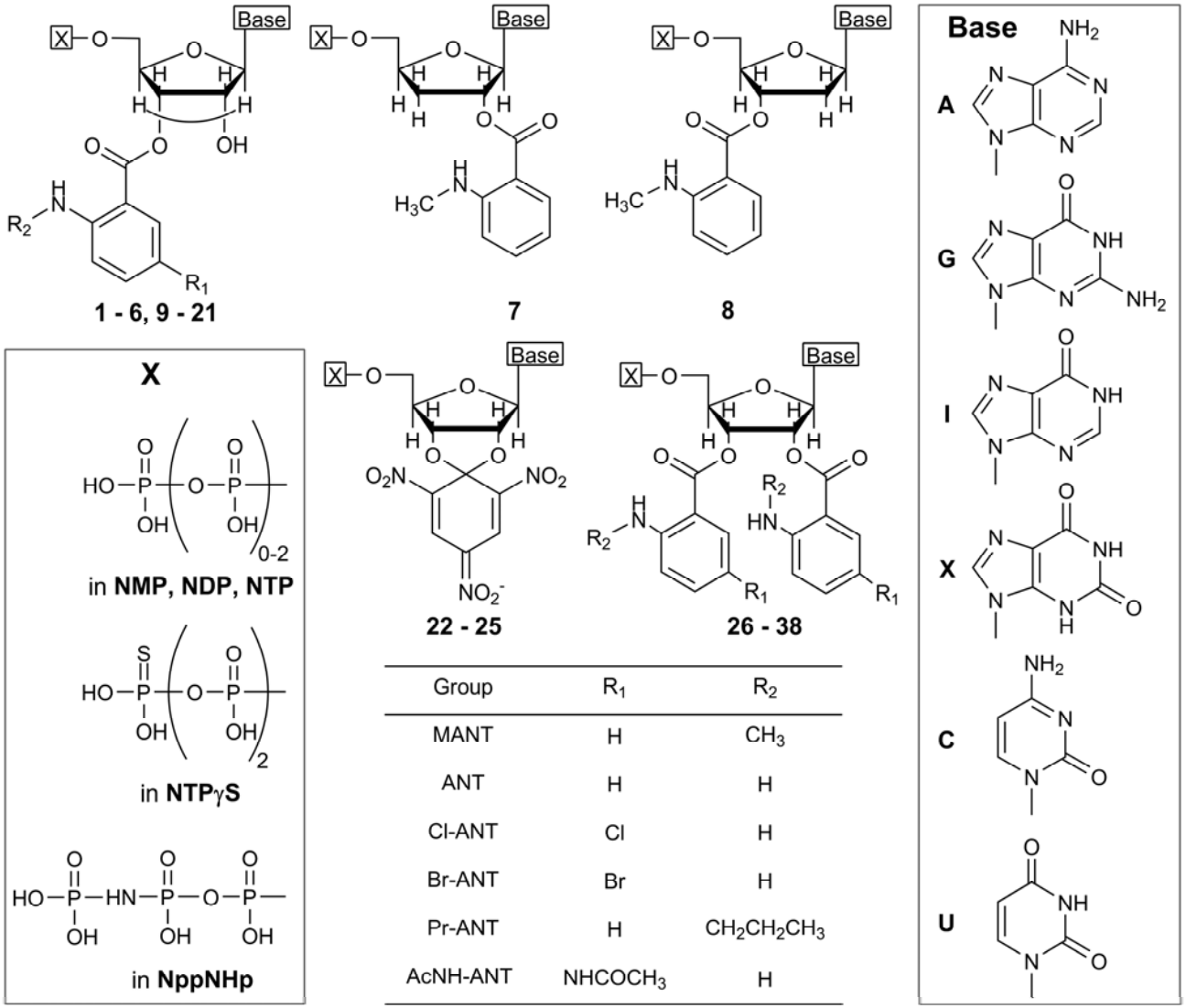

Group	R_1	R_2
MANT	H	CH_3
ANT	H	H
Cl-ANT	Cl	H
Br-ANT	Br	H
Pr-ANT	H	$CH_2CH_2CH_3$
AcNH-ANT	$NHCOCH_3$	H

Figure 2

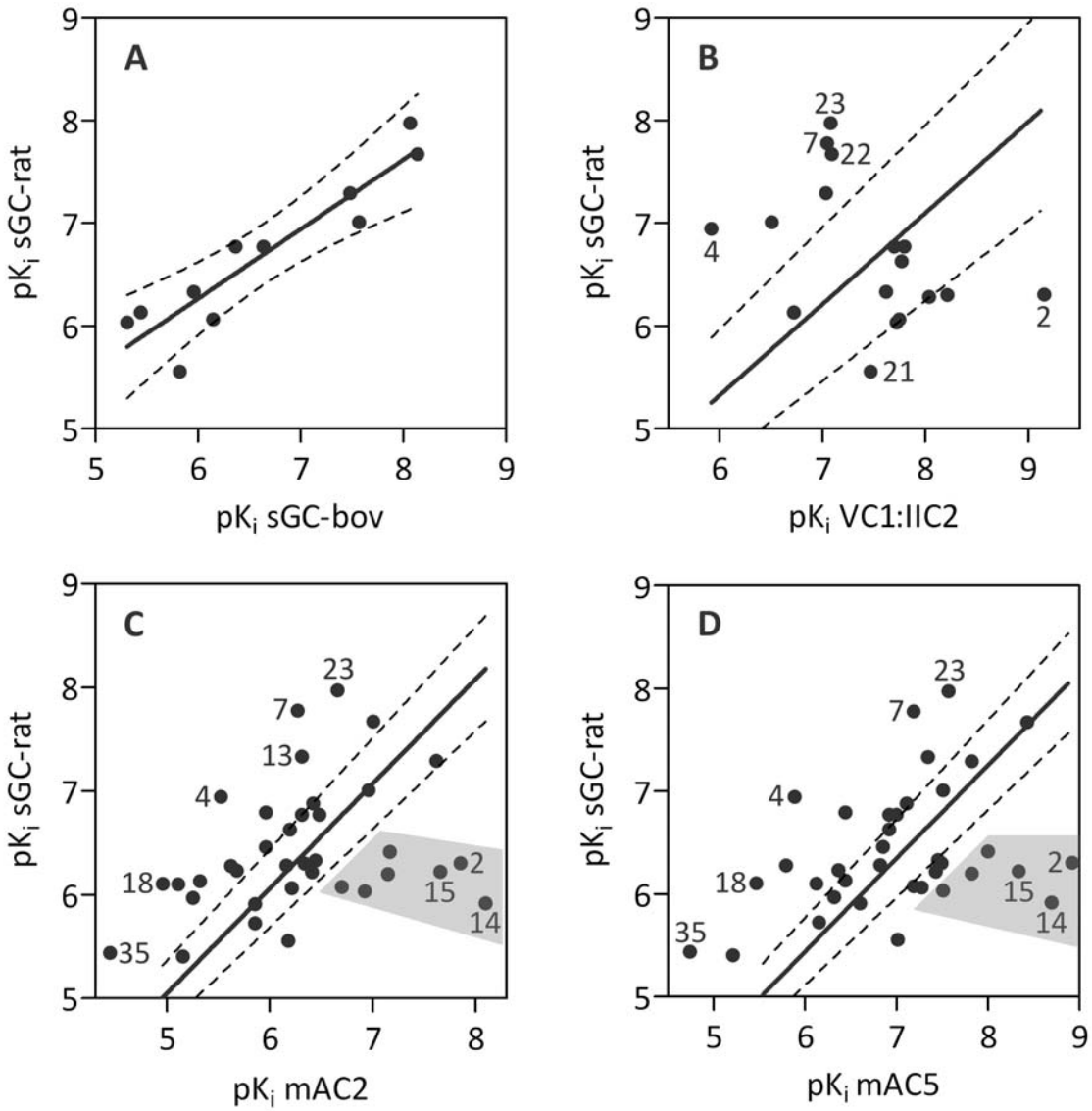

Figure 3

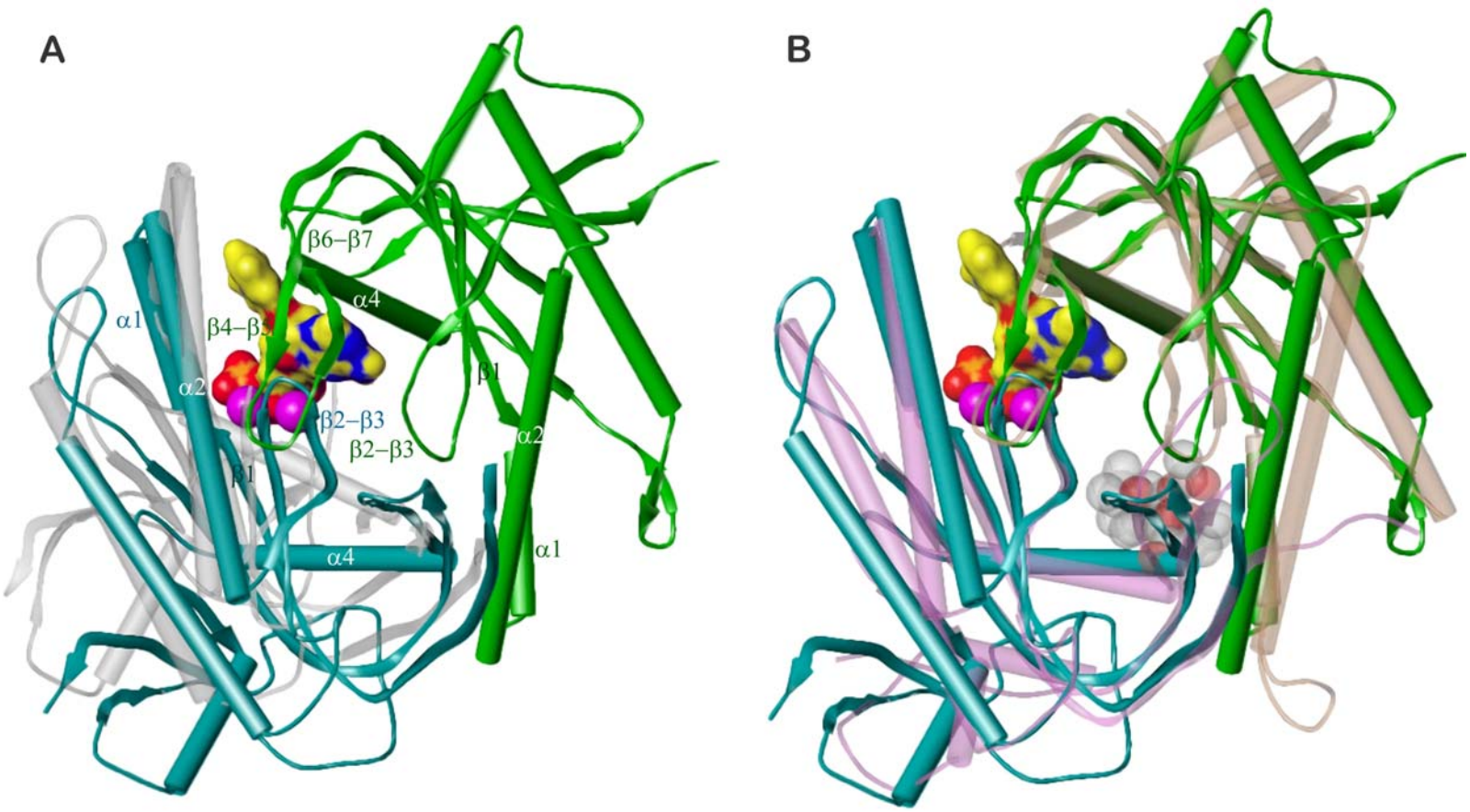

Figure 4